

Identification of wave systems in the multimodal sea state along the Indian shelf seas

M. M. Amrutha and V. Sanil Kumar*

Ocean Engineering Division, CSIR-National Institute of Oceanography (Council of Scientific & Industrial Research), Dona Paula 403004, Goa, India

*Corresponding author: sanil@nio.org

Abstract

The coexistence of multiple wave systems generated locally and by remote storms is common in the ocean and its quantification is required in the design of marine facilities. This study identifies the multi-modal sea states at six locations in the shelf seas of India based on partitioned wave output data from numerical model WAVEWATCH-III for 26 years (1990 to 2015). The different systems are identified by the propagation direction and frequencies with a relatively high probability of occurrence of spectral partitions. Four to seven types of distinct clusters of wave systems are present among the study locations. The occurrence of these systems and co-occurrence of this with other systems is examined. The southernmost location experiences the effect of seven wave systems. At all locations, two wave systems from the south with relatively low partial significant wave height (H_s) are present for more than 71% of time and co-occurred with other systems during 2-67%. The most energetic systems are observed 23 (system 5 at station 3)-60% (system 4 at station 4) of time with maximum mean partial H_s values of 1 to 3 m during summer monsoon months. The southernmost location (3) experienced maximum opposing (18%) and crossing (78%) sea states.

Keywords: North Indian Ocean, Probability Distribution of Spectral partitions, opposing and crossing seas, wind-sea, swell, WAVEWATCH-III

1. Introduction

Waves play an important role in many geophysical processes. The waves at a location are the result of atmospheric forcing having different spatial and temporal scales over the ocean. Multiple wave systems can coexist at the same location and time in the open ocean. Globally at different locations, 15-25% of the sea states consist of multiple wave systems (Boukhanovsky and Soares 2009). Understanding different wave systems at a location are crucial in studies related to air-sea interactions, wave modelling and design and deployment of wave energy converters and marine facilities. Different wave systems can be identified from the directional wave spectra showing energy distribution in frequency and direction using spectral partitioning techniques. The concept of spectral partitioning consists of identifying the relevant component or energy clusters from the entire wave spectrum, which implies the coexistence of waves generated locally, and by remote storms. Unimodal sea state can be represented easily by integrated bulk wave parameters, whereas there are serious shortcomings on the integrated wave parameters derived from multimodal sea state (Portilla 2018). In the case of multimodal sea states, the bulk wave parameters represent the mean wave direction and peak period of the wave system having higher energy. This issue can be easily tackled by spectral partitioning which allows understanding wave systems of different meteorological origins and it can provide a comprehensive view of local wave climate. Portilla (2018) presents the development of an open-access world atlas GLOSWAC (Global Spectral Wave Climate) based on the European Centre for Medium-Range Weather Forecasts (ECMWF) ERA-Interim containing spectral descriptors as a part of the study with long-term data of spectral clusters of a site in north Atlantic. The isolation of different wave systems in wave spectra are attempted at various geographical locations in the past (Gerling 1992; Hanson and Phillips 2001; Portilla et al. 2009). Recently, Echevarria et al. (2019) presented the global spectral wave climate at a resolution of $10^\circ \times 10^\circ$.

Besides the rich fishery resources, the shelf seas of India are potential sources for commercial exploration of hydrocarbon and falls in a busy navigational route. The waves in the Indian shelf seas, which is in the north Indian Ocean (NIO) are multimodal due to the influence of seasonally reversing monsoon winds, sea breeze, tropical cyclones, swells from the south Indian Ocean and the Atlantic Ocean (see George and Kumar 2020 and the references therein). Even though the two basins; the Arabian Sea (AS) and Bay of Bengal (BoB) of the north Indian Ocean separated by the Indian Peninsula are at the same latitudinal belt, they have distinct wave nature due to the geographical features, variation in wind field and arrival of swell field. Apart from these, waves in the western shelf seas are also influenced by the Findlater jet (Findlater 1969), Oman low-level jet, Shamal

winds (Aboobacker et al. 2011), Indian Ocean Dipole (Anoop et al. 2016), Makran winds (Anoop et al. 2020). In view of these, two locations each at eastern AS, western BoB and southern peninsular region are selected for the study. In the earlier studies on the wave spectral characteristics in the coastal waters of NIO (Dattatri et al. 1977; Narasimhan and Deo 1979; Kumar and Kumar 2008; Kumar et al. 2014; Anjali and Kumar 2016; Anjali and Kumar 2017), the integrated wave parameters are described and in some studies, wind-seas and swells are identified. However, the partitioning of the wave spectrum to identify multiple wave system is not attempted at many locations covering the Indian shelf seas. Hence, one of the objectives of the present study is to identify the multiple wave systems at few locations in the Indian shelf seas.

The interaction among the wave systems at a location is to be studied for estimating the impact on a structure or a hull when they have to face two (or more) wave trains coming from different directions. The multimodal seas and especially crossing seas have become famous because they are associated to ship accidents (Toffoli et al. 2005; Cavaleri et al. 2012). Toffali et al. (2005) mentioned the significance of standardized warning criteria based on ship accidents and they concluded that crossing seas might be dangerous to ships. Onorato et al. (2006) looked into the context of crossing sea state by introducing a plane wave propagating different directions with a single unstable plane wave. Onorato et al. (2006) speculated that the modulational instability of two wave trains with similar frequencies traveling at an angle could be responsible for the formation of freak/rogue waves. Research is still called for understanding the role of interaction between co-propagating wave trains for the occurrence of extreme waves (Toffali 2011). Bitner-Gregersen and Toffoli (2014) reported that in crossing seas extreme waves could occur for both narrow-banded and broad-banded directional spreading. Crossing waves, with special attention to the occurrence of freak waves, fall mostly into two main categories: the effect of a swell interacting with a wind-sea, and the interaction between two identical wave systems sharing the same carrier frequency (Trulsen et al. 2015). Hence, it is important to identify the opposing and crossing seas in the ocean. Quantification of the opposing and crossing seas in the Indian shelf seas is the second objective of the present study.

Motivated by the above facts, the present study is an attempt to identify and compute parameters of wave systems of different meteorological origins, which are independent of others in the Indian shelf seas based on the probability distribution of spectral partitions (PDS). Section 2 describes the data used in the study and the methodology. Results and discussion are presented in section 3 and the concluding remarks in section 4.

2. Data and methodology

WAVEWATCH-III (WWIII) numerical model version 4.18 (Tolman 1991) developed at NOAA/NCEP (National Centres for Environmental Prediction) is used for the simulation of waves. The multi-grid model simulation is carried out for 26 years from 1990 to 2015. Two model domains are considered, i) a big domain (75°S-35°N & 20°E-112°E) with a resolution of 0.5° covering the entire Indian Ocean and part of the Southern Ocean and ii) a small domain (5°N-25°N & 60°E-90°E) with a resolution of 0.1° (Figure 1a). The model is forced with ECMWF ERA5 wind (Hersbach and Dee 2016) with 1-h resolution and bathymetry data used is from ETOPO1 with a resolution of one arc min (Amante and Eakins 2009). The spectrum has 36 directional bins and 25 frequency bins spaced exponentially from 0.0412 to 0.4056 Hz. Different physics packages available in WWIII are described in the user manual (Tolman 2014). The different processes incorporated in the numerical model are; i) wave-wave interaction (non-linear interaction) which defines a third-generation model, ii) wind-wave interaction-dissipation term which should be considered as interrelated and balance between them governs the growth characteristics of the model, iii) shallow water process (wave-bottom interaction) to extremely shallow water processes (depth induced breaking, triad interaction) and different interaction of waves by bottom features (bottom-scattering), iv) wave-ice interaction and v) reflections offshore line or floating objects.

WWIII has different source term packages (ST1/2/3/4/6) based on the input-dissipation term. The older parameterizations ST1/2 are basically the least accurate ones. Some of the studies pointed out the uncertainties in determining the most accurate package among ST3/4/6 unambiguously (Liu et al. 2017). Amrutha et al. (2016) reported that among ST2 and ST4 simulations of WWIII with nested SWAN model domain, ST4 physics showed the best performance for a location in the eastern AS. Among different parameterization of ST2 and ST3, Seemanth et al. (2016) reported that BJA or ST3 simulation is better for the Indian Ocean irrespective of the seasons while for the pre-monsoon and northeast monsoon period ST2 simulation is good. Umesh and Behra (2019) reported that ST4 simulation is comparatively better even though for some stations, simulations using ST3 gave the best performance.

The wave fields, i.e., integrated parameters and the 2D spectra are saved at hourly intervals for the 26 years and used in the study. The model outputs of significant wave height (H_s) and energy period (T_e) which is one of the characteristic wave period derived from the wave spectrum is compared with the Datawell Directional Waverider buoy data. The two locations selected for the comparison are at the 15 m water depths off central eastern AS (Ratnagiri-16.980°N, 73.258° E) and Bay of Bengal (BoB) (Gopalpur-19.282°N, 84.964° E) for the year 2015. The inter-comparison of

model performance for H_s and T_e using the different input-dissipation terms (ST2/3/4) is shown with the help of a Taylor diagram (Figure 2) and the table of statistical parameters for model performance of the two locations. The Taylor diagram (Taylor 2001) can be used for a concise statistical summary of how well patterns match each other by means of their correlation, centered root-mean-square difference and standard deviation. The simulated and observed fields are in terms of good agreement when the distance between the fields is relatively short. Here for both the stations H_s and T_e simulations by ST2 physics is less reliable than ST3 or ST4, which perform more or less similar. Even though the ST4 simulation of H_s is a little better than ST3, The T_e simulation using ST3 is comparatively good than ST4. Hence, ST3 physics is used for further analysis of wave systems at six offshore locations.

The total energy represented by a 2D wave energy spectrum can be defined by bulk wave parameters. But there are spectral sub-features capable of giving more information regarding the energy situation at a particular location. The energy density spectrum with energy from sub-peaks within it can be considered as a topological surface. In such cases, it is logical to apply an image processing partition algorithm with partitions representing energy from sub-peaks within it. The wave systems are partitioned based on the digital image processing watershed algorithm (Vincent and Soille 1991) first prototyped by Hanson and Jensen (2004) for the analysis of ocean wave data. The scheme behind this method is to invert the spectral surface and spectral peaks to become catchments. The watershed (represent the minima) or boundaries of partitions can be determined by Vincent and Soille (1991) and the quantitative features of partitioned spectra are obtained. The long-term wave systems over a location are defined based on the number of partitions per spectral bin. The partitioned wave data from the model are extracted for six locations in the shelf seas of India (Figure 1b). Two locations are in the eastern AS at a water depth of 65 and 68 m, among which, one is at the north (station 1) and the other is at the central (station 2) eastern AS. Two locations each are selected at the southern peninsular region (stations 3 and 4) and western BoB (stations 5 and 6). The details of these stations are given in Table 1.

The interaction among multiple wave systems is categorized as opposing sea (in opposite direction with a range $\pm 45^\circ$) and crossing sea (wave trains with perpendicular direction in $\pm 45^\circ$ range). The balance wave systems will be following sea (travelling in the same direction within $\pm 45^\circ$). Small waves with $H_s < 0.5$ m are not considered while categorizing opposing and crossing waves. Waves are also classified into short (SP; $T_p < 7$ s), intermediate (IP; $7 \text{ s} \leq T_p \leq 14$ s) and long (LP; $T_p > 14$ s) period and their percentage of occurrences are calculated.

Long-term extreme values of wave heights are typically estimated using extreme value theory. Extreme value analysis is carried out by following the Generalized Extreme Value (GEV) distribution model with annual maximum values (Goda 1992). Estimate based on annual maximum values is the common approach to ensure that the dataset truly represents extreme values and that the data are independent (Takbash and Young 2019).

The Indian shelf seas experience three different seasons: pre-monsoon (February-May), summer monsoon/southwest monsoon (June-September) and northeast monsoon (October-January). Accordingly, seasonal characteristics are presented.

3. Results and discussion

3.1 Wave characteristics at the study locations

At the study locations, the H_s ranges from 0.3 to 8.8 m and station 1 has the highest H_s . Wave heights are relatively high in the northern AS (station 1) and central west coast of India (station 2) and in the northern BoB (station 6). The maximum H_s at stations 3 and 4 are low with values of 3.7 m and 3.3 m (Table 1). However, the 50th percentile H_s is highest at stations 3 and 4 with values of 1.55 m and 1.33 m. Among the other stations, the 50th percentile of H_s ranged from 1.12 m at station 5 to 1.31 m at station 6. Even though H_s up to 8.8 m is occurring at station 1, only 10% of the time H_s exceeded 2.89 m and 1% of the time H_s exceeded 4.11 m (Table 1). 100-year return level value is also high at stations 1 and 6 (8.56 m and 8.50 m) and low at stations 3 and 4 (3.73 m and 3.26 m). Since station 4 is in the Gulf of Mannar and partially covered by Sri Lankan landmass, relatively low wave heights are observed at this station.

3.2. Characteristics of multiple wave systems

The possible genesis of the wave system can be estimated by the propagation direction and peak frequencies. The details of different wave systems with distinct directional and peak frequency range present at all six locations are given in Figure 3. The different wave systems identified are numbered randomly. The PDS indicated by the color bar in Figure 3 gives the percentage occurrence of different wave systems. The magnitude of the density distribution of partitions varies with the datasets, which have different time and spectral resolutions. From the available partitioned wave output data, it is observed that southern station 3 is influenced by seven wave systems having different characteristics. At all the locations, the presence of two swell systems from the south with low directional spreading is observed throughout the year. These two systems differ slightly in their period, but are in a different direction and height, which indicates that these systems might have different generation sources.

Details of partial wave height distribution of individual wave systems are represented in the box-whisker plot (Figure 4) and the box indicates the 25th and 75th percentile range (Inter Quartile Range). The whiskers are placed at 1.5 times of interquartile range from the 1st and 3rd quartile values. The outliers falling above this whisker is considered as extremes or tail of the distribution and are given in red dots. The mean, maximum and 50th, 90th and 99th percentile H_s of different wave systems are presented in Table 2. At every station, the highly recurrent systems are from the south with a relatively low magnitude of waves and are observed 22.0 to 44.6% among the occurrence of waves from different wave system. There are other wave systems present with a low magnitude of H_s such as system 6 at stations 1 and 3 and system 2 at stations 5 and 6. The systems with relatively high magnitudes are system 2 (at stations 1 and 2), systems 5 and 7 (at station 3), system 4 (at station 4) and system 5 (at stations 5 and 6) during 5.25 to 18.23% of the time. These systems have a relatively less number of waves with extreme partial H_s . Among the stations studied, the most energetic system is observed 24% (system 5 at station 3) to 60% of the times (system 4 at station 4).

100-year return level H_s for systems 4 and 5 at station 1 is highest with values of 9.54 m and 9.43 m and the next highest value (8.49 m) is for system 4 at station 6. At station 2, system 2 has a 100-year return level of 7.10 m and at station 5; system 3 has 6.75 m (Table 2).

At the locations in the western shelf sea, the most energetic system 2 is with frequency ≤ 0.15 Hz and a direction range of 220-270°. At stations 1 and 2, system 2 and 3 are due to the summer monsoon winds, system 1 is due to shamal and Makran winds and systems 4 and 5 are the swells from the south. For southern station 3, the strongest are systems 5 and 7 and are from 260-300°. At station 4, the strongest system 4 is from 210-240°. In the eastern shelf sea locations, the strongest is system 5 and is from 180-210°. The strongest system at all stations is with H_s mean value of 1 to 3 m during the summer monsoon months (Figure 5).

A widespread system from a direction range 270-360° with comparatively high frequency (0.15 to 0.2 Hz) is present at locations in the western shelf sea and the same system is present at southern location 3 in a narrow directional sector (between 290 and 330°). A high-frequency system (system 1) is present in 45-90° at southern locations 3 and 4. These systems are absent during summer monsoon months and have a maximum monthly mean partial H_s values from December to February (Figure 5) indicating that influenced by northeasterly winds. The occurrence of these systems is possible either alone or together which contributes to the total characteristics.

The details of wave systems with the short-wave period (SP), intermediate-wave period (IP) and long-wave period (LP) occurrence is given in Table 3. The strongest system of locations in the

western shelf sea, IP is observed throughout system 2. The two systems (systems 5 and 7) present at southern location 3 are with comparatively the same mean partial H_s and different period category. System 5 is of IP and system 7 consists of SP (86.1%) and IP (13.9%). In the case of station 4, 92% of the time, system 4 consists of SP. For locations in the eastern shelf sea, system 5 is present with SP to IP waves and also another system (system 3 of station 5 and system 4 of station 6) of IP is present with comparable H_s . H_s of the resultant wave (total H_s) median is higher than the median of all the systems present for locations 3 to 6. Among the two most occurring systems from the southern direction, 97.7-100% of one system consists of IP for all the stations. Another system of southern direction composed of LP and IP with the maximum percentage of LP occurrence found at east coast locations (88.9%-90.6%) than southernmost (46.7%-55.7%) and west coast (31.5%-33.3%) locations.

Figure 6 represents the details of location wise occurrence of a system in the first column and co-occurrence of it with other systems in the upper half of each table for the period of study. Among the wave systems, two systems within a direction range of $135-225^\circ$ and a period greater than 6 s from the south Indian Ocean are the most occurred systems (>86% of times) for all the stations except station 5 with >71% of times. These two systems present each other 67% of the times at station 5 and more than 80% of the times for the rest of the stations. The co-occurrence of these southerly systems with other systems for station 1 is having a range of 5% (system 6) to 53% (system 1). System 6 is a less observed one, which occurred nearly 5% of the time. In station 2, these systems co-occurred 11% (system 3) to 67% (system 1) of the times with other systems. The most energetic system 2 at stations 1 and 2 appears 24-31% times with the southerly systems. System 3 present at locations in western shelf sea has the same directional range but comparatively lower period than system 2, and are observed 11-17% of the times co-occurred with the southerly systems. In the case of station 3, systems 5 and 7 are observed with the southerly systems almost all the time when they present individually (23 and 37%). 53-55% of times the co-occurrence of the two-southerly systems with the higher energy system 4 is observed at station 4. There are three systems present at stations 5 and 6 within $135-225^\circ$ among which systems 3 and 4 are the most observed ones (71-96%). System 5 of locations in the eastern shelf sea present 34-37% of the times and co-existed 25-35% of times with the other two southerly systems.

At all locations in the Indian shelf seas, swells having an intermediate period and long period dominates and only at station 2, apart from swells, wind-seas (system 1) is also predominant. Even though multiple wave systems were not analysed, earlier studies on wind-seas and swells in the

Indian shelf seas also identified swell dominance at most locations (Naseef and Kumar 2020) and dominance of wind-seas and swells in the central west coast of India (Kumar et al. 2014).

3.3 Crossing and opposing seas

The details of the total occurrence of crossing and opposing seas are given in Table 4 and the percentage occurrence of the same among two systems is given in the lower half of the table for each location in Figure 6. Locations in the western shelf seas (stations 1 and 2) experience mainly crossing sea states 54 and 36% of times and opposing sea states were only 1.36 and 9.65% of times. In the western shelf seas, mainly systems 1 and 4 crosses i.e., wind-sea and swell with mean H_s of 0.5 m. At station 2, apart from wind-seas and swells crossing, a significant period of time (25%), two swells cross each other (systems 2 and 4) having mean H_s of 2.15 m and 0.46 m (Table 2 and Figure 6).

The total occurrence of opposing sea states at locations in the eastern shelf sea is less than 0.24% of the times and crossing sea states are occurring 9.49 to 16.08% of the times, which indicates that mostly following seas are in the eastern shelf seas. Southern locations are having a maximum (69.8-77.9% of times) crossing sea state. 17.8% of the time opposing sea states occurred among different systems present at station 3. Being in the Gulf of Mannar, station 4 has also fewer opposing sea states (<0.12% of times). Mostly the swells are crossing the wind-seas at all stations. At station 3, apart from wind-seas crossing the swells, swells having mean H_s of 0.74 m are crossing swells having mean H_s of 0.51 m (Table 2 and Figure 6).

Most of the crossing seas are during the summer monsoon period at stations 3 and 4, whereas at station 1 in the western shelf sea, crossing seas are high during the pre-monsoon period due to the presence of northwesterly waves and southerly swells. At station 2, crossing sea states observed are maximum during the summer monsoon period. In the eastern shelf seas, crossing seas are relatively high during the northeast monsoon period (Table 4). At the southernmost location (station 3), the opposing seas are high during the summer monsoon period. In the western shelf seas, opposing seas are mainly during the non-monsoon period.

The difference in the opposing and crossing sea state statistics with smaller data sets (6 years from 2010 to 2015) is examined with larger datasets (26 years from 1990 to 2015). The percentage difference between the total occurrence of opposing sea state among systems with smaller data sets and larger data sets varies considerably. There is no significant difference observed for stations 3 and 5, while an increase of 13% and 50% is noticed for stations 2 and 6 respectively and a reduction of 43% is noted for station 4. Whereas, total crossing sea state of station 1 shows an increase of 7.3%

and a reduction of 9.9% at station 5. The study emphasizes the importance of analyzing long-term wave data before reporting the wave climate for a location.

4. Concluding remarks

The study based on the 26 years wave hindcast data obtained from a validated numerical model shows that the multi-modal sea states are common at all six locations along the shelf seas of India. Four to seven types of distinct clusters of wave systems are present among the locations of study with a maximum number of seven wave systems present at the southern location (station 3). The two most observed wave systems (>71% of times) at every location are from the south direction bearing a relatively low magnitude of partial H_s . The co-occurrence of this system with other systems present at different stations varies from 2 to 67% of the time. The strongest system at all stations is with H_s mean value of 1 to 3 m during the summer monsoon months. The most energetic system in the western shelf sea (system 2) and a southern location (system 5) are of intermediate wave period. At all locations, swells having an intermediate period and long period dominates and only at station 2, wind-seas (system 1) is also predominant. The crossing sea states in the western shelf sea are 36.2 to 54.5%. The percentage of opposing sea states at all locations varies from 0.02 (station 5) to 17.77% (station 3). Southern locations are having a maximum (69.7-77.4%) crossing sea state.

Acknowledgments

The authors acknowledge the financial support given by the Council of Scientific & Industrial Research, New Delhi (CSIR), to conduct this research and Director, CSIR-NIO for facilities. First author wishes to acknowledge CSIR for the award of Senior Research Fellowship. ERA5 wind data used in this study is obtained from the ECMWF data server: <http://data.ecmwf.int/data>. . The authors thank the reviewers for the comments and suggestions, which improved the scientific content of the paper. This work is a part of the Doctoral thesis of the first author registered with Bharathidasan University, Tiruchirappalli and bears NIO contribution ----

Reference

- Aboobacker VM, Vethamony P, Rashmi R (2011) “Shamal” swells in the Arabian Sea and their influence along the west coast of India. *Geophys. Res. Lett.* 38 (3): L03608. <https://doi.org/10.1029/2010GL045736>.
- Amante C, Eakins B (2009) ETOPO1 1 Arc-Minute Global Relief Model: Procedures, Data Sources and Analysis. NOAA Technical Memorandum NESDIS, NGDC-24, 19 pp
- Amrutha MM, Kumar VS, Sandhya KG, Nair TMB, Rathod JL (2016) Wave hindcast studies using SWAN nested in WAVEWATCH III - comparison with measured nearshore buoy data off Karwar, eastern Arabian Sea, *Ocean Engineering* 119C: 114-124. [10.1016/j.oceaneng.2016.04.032](https://doi.org/10.1016/j.oceaneng.2016.04.032).
- Anjali NM, Kumar VS (2016) Spectral wave climatology off Ratnagiri, northeast Arabian Sea. *Natural Hazards* 82: 1565-1588. [https://doi: 10.1007/s11069-016-2257-5](https://doi.org/10.1007/s11069-016-2257-5)
- Anjali NM, Kumar VS (2017) Wave spectral shapes in the coastal waters based on measured data off Karwar on the western coast of India. *Ocean Science* 13: 365-378. [https://doi: 10.5194/os-2016-91](https://doi.org/10.5194/os-2016-91)
- Anoop TR, Kumar VS, Shanas PR, Johnson Glejin, Amrutha MM (2016) Indian Ocean Dipole modulated wave climate of eastern Arabian Sea. *Ocean Sci.* 12: 369–378. <https://doi.org/10.5194/osd-12-2473-2015>
- Anoop TR, Shanas PR, Aboobacker VM, Sanil Kumar V, Nair LS, Prasad R, Reji S (2020) On the generation and propagation of Makran swells in the Arabian Sea. *Int. J. climatology* 40 (1): 585–593. <https://doi.org/10.1002/joc.6192>
- Bitner-Gregersen EM, Toffoli A (2014) Occurrence of rogue sea states and consequences for marine structures. *Ocean Dynamics* 64(10): 1457-1468
- Boukhanovsky AV, Soares CG (2009) Modelling of multi peaked directional wave spectra. *Appl. Ocean Res.* 31: 132–141
- Cavaleri L, Bertotti L, Torrisi L, Bitner-Gregersen E, Serio M, Onorato M (2012) Rogue waves in crossing seas: The Louis Majesty accident, *J. Geophys. Res.* 117: C00J10, [https://doi:10.1029/2012JC007923](https://doi.org/10.1029/2012JC007923).
- Dattatri J, Raman H, Shankar NJ (1977) Comparison of Scott spectra with ocean wave spectra. *Journal of the Waterway, Port, Coastal and Ocean Division* 103: 375-378
- Echevarria ER, Hemer MA, Holbrook NJ (2019) Seasonal variability of the global spectral wind-wave climate. *J. Geophys. Res. Oceans* 124: 2924–2939, <https://doi.org/10.1029/2018JC014620>
- Findlater J (1969) A major low-level air current near the Indian Ocean during the northern summer. *Quart. J. Roy. Meteor. Soc.* 95 (404): 362–380. [https://doi.org/ 10.1002/qj.49709540409](https://doi.org/10.1002/qj.49709540409)
- George J, Kumar VS (2020) Climatology of wave period in the Arabian Sea and its variability during the recent 40 years, *Ocean Engineering* 216: Article number 108014, <https://doi.org/10.1016/j.oceaneng.2020.108014>
- Gerling TW (1992) Partitioning sequences and arrays of directional ocean wave spectra into component wave systems. *Journal of atmospheric and Oceanic Technology* 9(4): 444-458

- Goda Y (1992) Uncertainty of design parameters from viewpoint of extreme statistics, *J Offshore Mech Arct.* 114(2): 76-82
- Hanson JL, Jensen RE (2004) Wave system diagnostics for numerical wave models. In 8th International Workshop on Wave Hindcasting and Forecasting, Oahu, Hawaii, pp. 231-238
- Hanson JL, Phillips OM (2001) Automated analysis of ocean surface directional wave spectra. *Journal of atmospheric and oceanic technology* 18(2): 277-293
- Hersbach H, Dee D (2016) ERA5 reanalysis is in production. *ECMWF Newsletter* 2016, 147.7. <https://www.ecmwf.int/en/newsletter/147/news/era5-reanalysis-production>
- Kumar VS, Dubhashi KK, Nair TMB (2014) Spectral wave characteristics off Gangavaram, Bay of Bengal. *Journal of Oceanography* 70: 307-321. <https://doi.org/10.1007/s10872-014-0223-y>
- Kumar VS, Kumar KA (2008) Spectral characteristics of high shallow water waves. *Ocean Engineering* 35: 900-911. <https://doi: 10.1016/j.oceaneng.2008.01.016>
- Liu Q, Babanin A, Fan Y, Zieger S, Guan C, Moon IJ (2017) Numerical simulations of ocean surface waves under hurricane conditions: Assessment of existing model performance. *Ocean Modelling* 118: 73-93
- Naseef TM, Sanil Kumar V (2020) Climatology and trends of the Indian Ocean surface waves based on 39-year long ERA-5 reanalysis data. *Int J Climatol* 40:979–1006. <https://doi.org/10.1002/joc6251>
- Narasimhan S, Deo MC (1979) Spectral analysis of ocean waves-a study. *Proceedings of the conference on civil engineering in oceans, Vol 1, ASCE, New York, 877–892*
- Onorato M, Osborne AR, Serio M (2006) Modulational instability in crossing sea states: A possible mechanism for the formation of freak waves. *Physical review letters* 96(1): 014503
- Portilla J, Ocampo-Torres FJ, Monbaliu J (2009) Spectral partitioning and identification of wind sea and swell. *Journal of atmospheric and oceanic technology* 26(1): 107-122
- Portilla J (2018) Open Access Atlas of Global Spectral Wave Conditions Based on Partitioning. *Proceedings of the ASME 2018 37th International Conference on Ocean, Offshore and Arctic Engineering. Volume 11B: Honoring Symposium for Professor Carlos Guedes Soares on Marine Technology and Ocean Engineering. Madrid, Spain. June 17–22, 2018. V11BT12A051. ASME.* <https://doi.org/10.1115/OMAE2018-77230>
- Seemanth M, Bhowmick SA, Kumar R, Sharma R (2016) Sensitivity analysis of dissipation parameterizations in a third-generation spectral wave model, WAVEWATCH III for Indian Ocean. *Ocean Engineering* 124: 252-273
- Takbash A, Young IR (2019) Global ocean extreme wave heights from spatial ensemble data. *Journal of Climate* 32: 6823-6836
- Taylor KE (2001) Summarizing multiple aspects of model performance in a single diagram. *Journal of Geophysical Research: Atmospheres* 106(D7): 7183-7192
- Toffoli A, Lefevre JM, Bitner-Gregersen E, Monbaliu J (2005) Towards the identification of warning criteria: analysis of a ship accident database. *Applied Ocean Research* 27(6): 281-291

Toffoli A, Bitner-Gregersen EM, Osborne AR, Serio M, Monbaliu J, Onorato M (2011) Extreme waves in random crossing seas: Laboratory experiments and numerical simulations. *Geophysical Research Letters* 38: L06605, doi:10.1029/2011GL046827

Tolman HL (1991) A third-generation model for wind waves on slowly varying, unsteady and inhomogeneous depths and currents. *J. Phys. Oceanogr.* 21: 782–797

Tolman HL (2014) User manual and system documentation of WAVEWATCH III® version 4.18, NOAA Technical Note, MMAB Contribution No. 316

Trulsen K, Nieto Borge JC, Gramstad O., Aouf L, Lefe`vre J.–M (2015) Crossing sea state and rogue wave probability during the Prestige accident, *J. Geophys. Res. Oceans* 120: 7113–7136, doi:10.1002/2015JC011161

Umesh PA, Behera MR (2020) Performance evaluation of input-dissipation parameterizations in WAVEWATCH III and comparison of wave hindcast with nested WAVEWATCH III-SWAN in the Indian Seas. *Ocean Engineering* 202: article number 106959. <https://doi.org/10.1016/j.oceaneng.2020.106959>

Vincent L, Soille P (1991) Watersheds in digital spaces: an efficient algorithm based on immersion simulations. *IEEE Transactions on Pattern Analysis & Machine Intelligence* 6: 583-598

Table 1. Details of the study locations and the wave parameters during 1990-2015

Station number	Location	Water depth (m)	Distance from the coast (km)	Significant wave height (m)					Peak period range (s)	Direction range (degree)
				range	50 th percentile	90 th percentile	99 th percentile	100-yr return level		
1	21.00° N; 69.50° E	65	54	0.3-8.8	1.15	2.89	4.11	8.56	2.7-21.9	0-360
2	16.50° N; 72.75° E	68	60	0.4-6.7	1.20	2.77	4.00	7.10	3.5-22.0	4-360
3	07.75° N; 77.25° E	61	42	0.6-3.7	1.55	2.38	2.91	3.73	4.4-22.0	29-297
4	08.25° N; 78.25° E	28	24	0.4-3.3	1.33	1.83	2.21	3.26	2.7-22.0	2-310
5	16.75° N, 82.50° E	99	16	0.4-5.5	1.12	1.60	2.19	5.84	3.4-22.0	45-286
6	20.00° N; 86.75° E	58	30	0.3-7.4	1.31	2.13	3.02	8.50	3.0-22.0	12-328

Table 2. 50th , 90th and 99th percentile significant wave height of various systems present at the study locations 1 to 6 along with mean, maximum and 100-year return level

Significant wave height (m)						
System	mean	50th percentile	90th percentile	99th percentile	maximum m	100_yr_return level
Station 1						
1	0.54	0.50	0.91	1.32	3.32	3.55
2	2.28	2.28	3.53	4.45	6.79	7.10
3	0.73	0.63	1.41	2.07	3.24	3.08
4	0.44	0.38	0.80	1.24	8.75	9.54
5	0.31	0.28	0.49	0.86	8.25	9.42
6	0.22	0.19	0.35	0.63	1.47	1.67
Station 2						
1	0.57	0.52	0.99	1.45	2.98	3.49
2	2.15	2.15	3.42	4.36	6.70	7.10
3	0.52	0.44	0.96	1.64	2.93	3.20
4	0.46	0.40	0.83	1.24	4.30	5.86
5	0.35	0.33	0.52	0.73	4.24	5.66
Station 3						
1	0.86	0.85	1.43	1.81	2.37	2.44
2	0.74	0.72	1.13	1.49	2.09	2.10
3	0.51	0.40	1.02	1.67	2.67	2.91
4	0.51	0.35	1.20	2.01	3.57	4.44
5	1.35	1.40	2.17	2.75	3.50	3.56
6	0.26	0.22	0.43	0.97	1.99	1.96
7	1.10	1.08	1.91	2.49	3.32	3.33
Station 4						
1	0.89	0.91	1.36	1.66	2.79	2.84
2	0.67	0.65	0.99	1.33	1.90	2.06
3	0.43	0.34	0.84	1.46	3.05	2.99
4	1.00	1.06	1.53	1.92	2.98	3.19
Station 5						
1	0.62	0.54	1.17	1.89	3.46	3.20
2	0.42	0.36	0.74	1.55	3.00	3.45
3	0.68	0.62	1.22	1.80	5.51	6.75
4	0.31	0.24	0.59	1.19	2.26	2.39
5	0.81	0.81	1.32	1.65	2.97	3.57
Station 6						
1	0.44	0.38	0.79	1.39	2.80	3.05
2	0.35	0.25	0.66	1.56	2.72	3.18
3	0.45	0.36	0.85	1.46	3.64	4.16
4	0.78	0.61	1.66	2.73	7.40	8.49
5	0.97	0.95	1.66	2.19	3.29	3.34

Table 3. Percentage of short (SP; $T_p < 7s$), intermediate (IP; $7s \leq T_p \leq 14s$) and long (LP; $T_p > 14s$) period waves in different wave systems at each station

System number	Wave type	Station number					
		1	2	3	4	5	6
1	SP	96.35	95.16	99.29	99.96	94.83	98.61
	IP	3.65	4.84	0.71	0.04	5.17	1.39
	LP	-	-	-	-	-	-
2	SP	-	-	-	0.12	70.11	93.52
	IP	99.89	99.99	98.90	99.88	29.89	6.48
	LP	0.11	0.01	1.10	-	-	-
3	SP	59.62	55.11	-	-	-	-
	IP	40.38	44.89	53.31	44.26	100.00	11.11
	LP	-	-	46.69	55.74	-	88.89
4	SP	-	-	61.57	91.63	-	-
	IP	66.69	68.51	38.43	8.37	9.45	100.00
	LP	33.31	31.49	-	-	90.55	-
5	SP	-	-	-	-	61.73	69.21
	IP	97.65	99.78	99.98	-	38.27	30.79
	LP	2.35	0.22	0.02	-	-	-
6	SP	100.00	-	93.64	-	-	-
	IP	-	-	6.36	-	-	-
	LP	-	-	0.00	-	-	-
7	SP	-	-	86.06	-	-	-
	IP	-	-	13.94	-	-	-
	LP	-	-	0.00	-	-	-

Table 4. Season wise percentage occurrence of opposing and crossing seas among the systems present at a location. Waves with significant wave height less than 0.5 m are not considered in the analysis

Station No.	Percentage of							
	Opposing seas				Crossing seas			
	Total	Pre- monsoo n	Summer monsoon	Northeas t monsoon	Total	Pre- monsoo n	Summer monsoon	Northeast monsoon
1	1.36	0.62	0.12	0.63	36.16	18.19	11.23	6.74
2	9.65	4.42	0.58	4.64	54.49	18.14	27.41	8.95
3	17.77	5.74	9.97	2.06	77.88	19.87	32.64	25.37
4	0.12	0.00	0.00	0.12	69.83	17.69	31.71	20.43
5	0.02	0.00	0.02	0.00	16.08	1.72	0.46	13.91
6	0.24	0.04	0.09	0.11	9.49	3.03	0.81	5.65

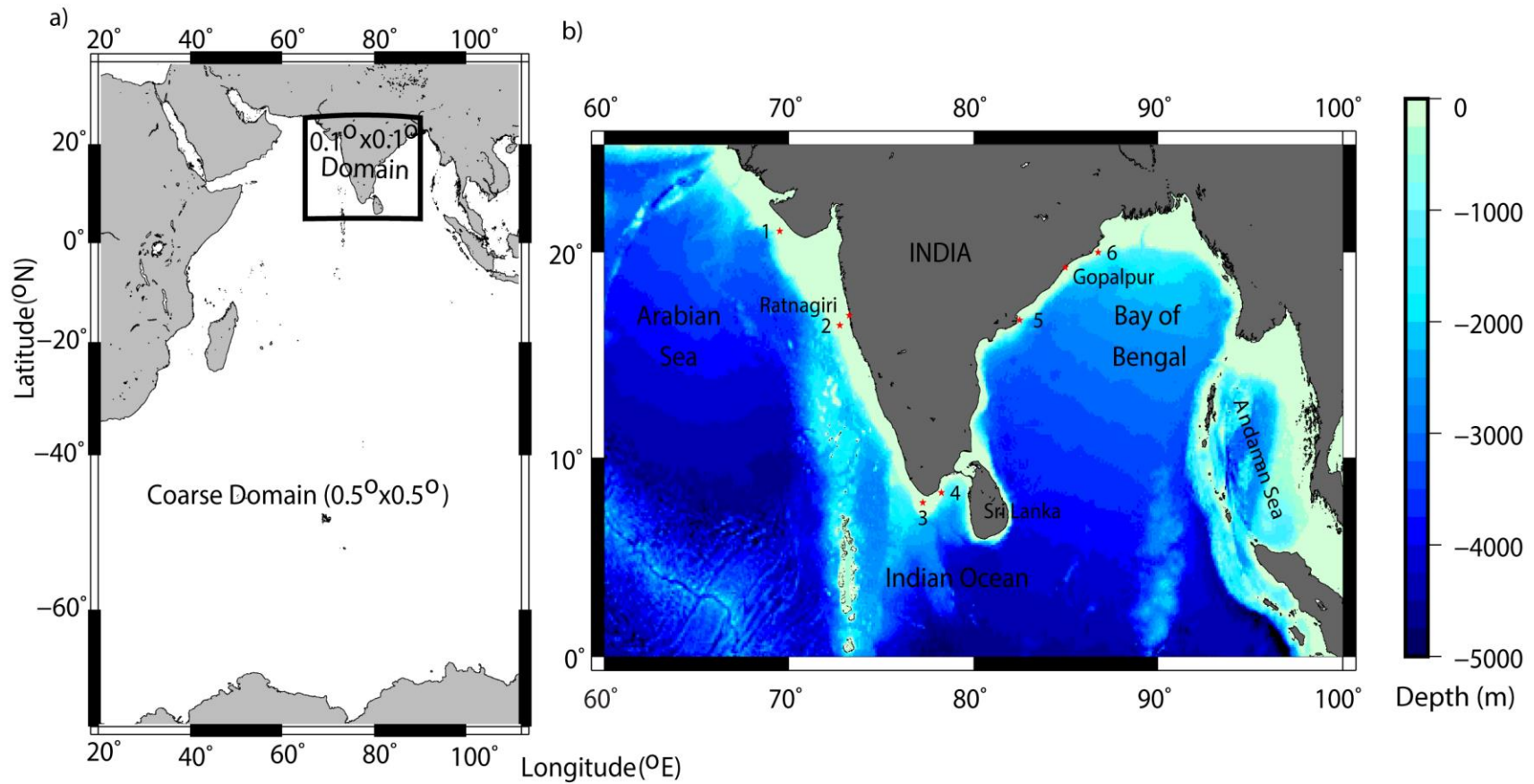
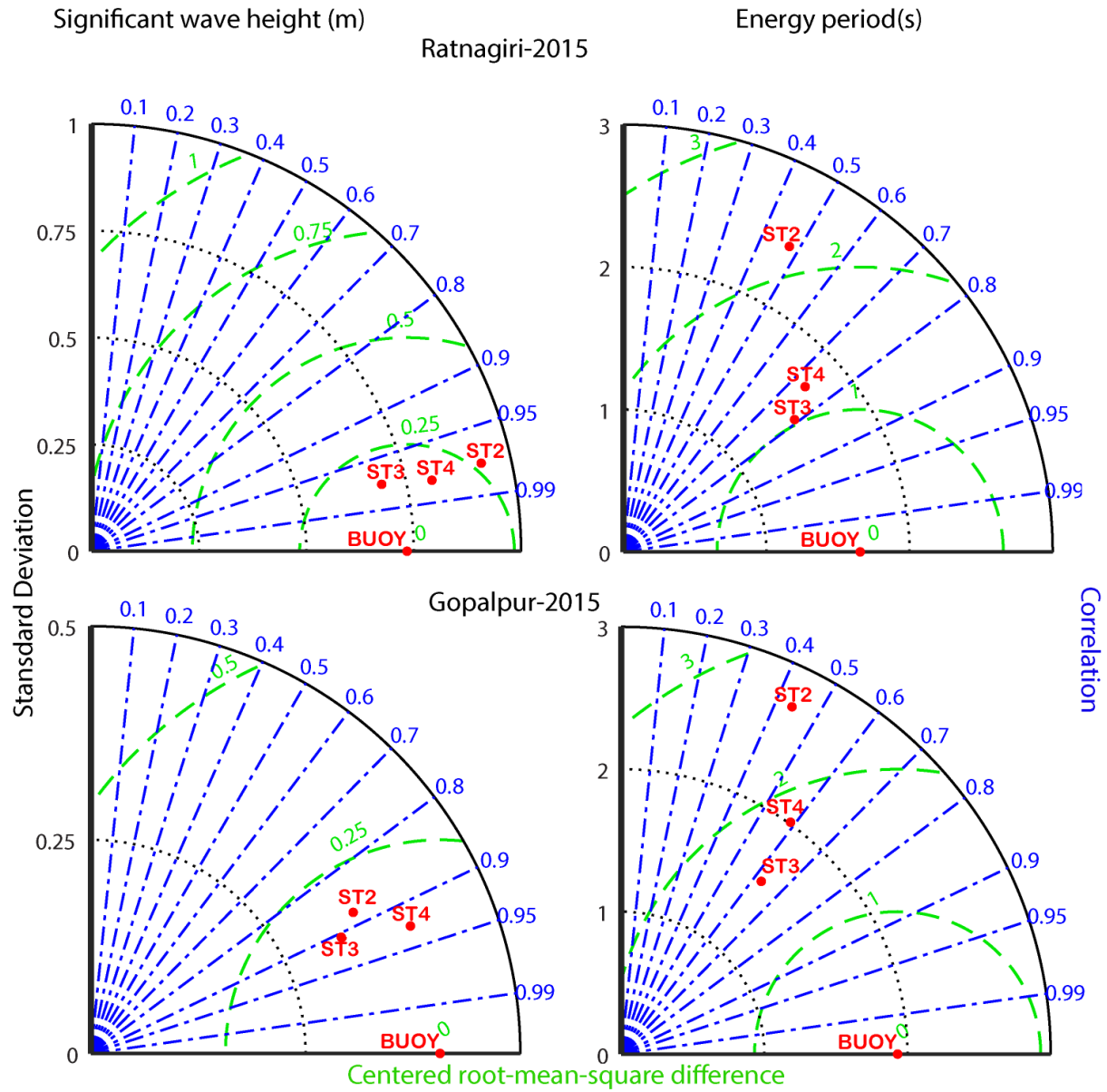


Figure 1..a) Multi-model grid domain of numerical model WWIII, b) Six locations considered in the present study in the north Indian Ocean; 1 to 6 are marked as dots. Measured buoy data used for model validations are from Ratnagiri and Gopalpur. The colour shade is the depth contour based on ETOP1 (Amante and Eakins 2009)



Station		ST2			ST3			ST4		
		Bias	Corr	RMSE	Bias	Corr	RMSE	Bias	Corr	RMSE
Ratnagiri	H _s	0.02	0.98	0.27	0.09	0.97	0.19	-0.02	0.98	0.18
	T _e	1.61	0.53	2.54	1.04	0.79	1.47	1.24	0.74	1.74
Gopalpur	H _s	0.08	0.89	0.2	0.03	0.91	0.18	-0.09	0.93	0.18
	T _e	3.65	0.44	4.45	0.43	0.63	1.6	0.84	0.59	1.98

Figure 2. Taylor diagram for comparison of significant wave height (H_s in meters) and energy period (T_e in seconds) from WWIII model output with measured buoy data

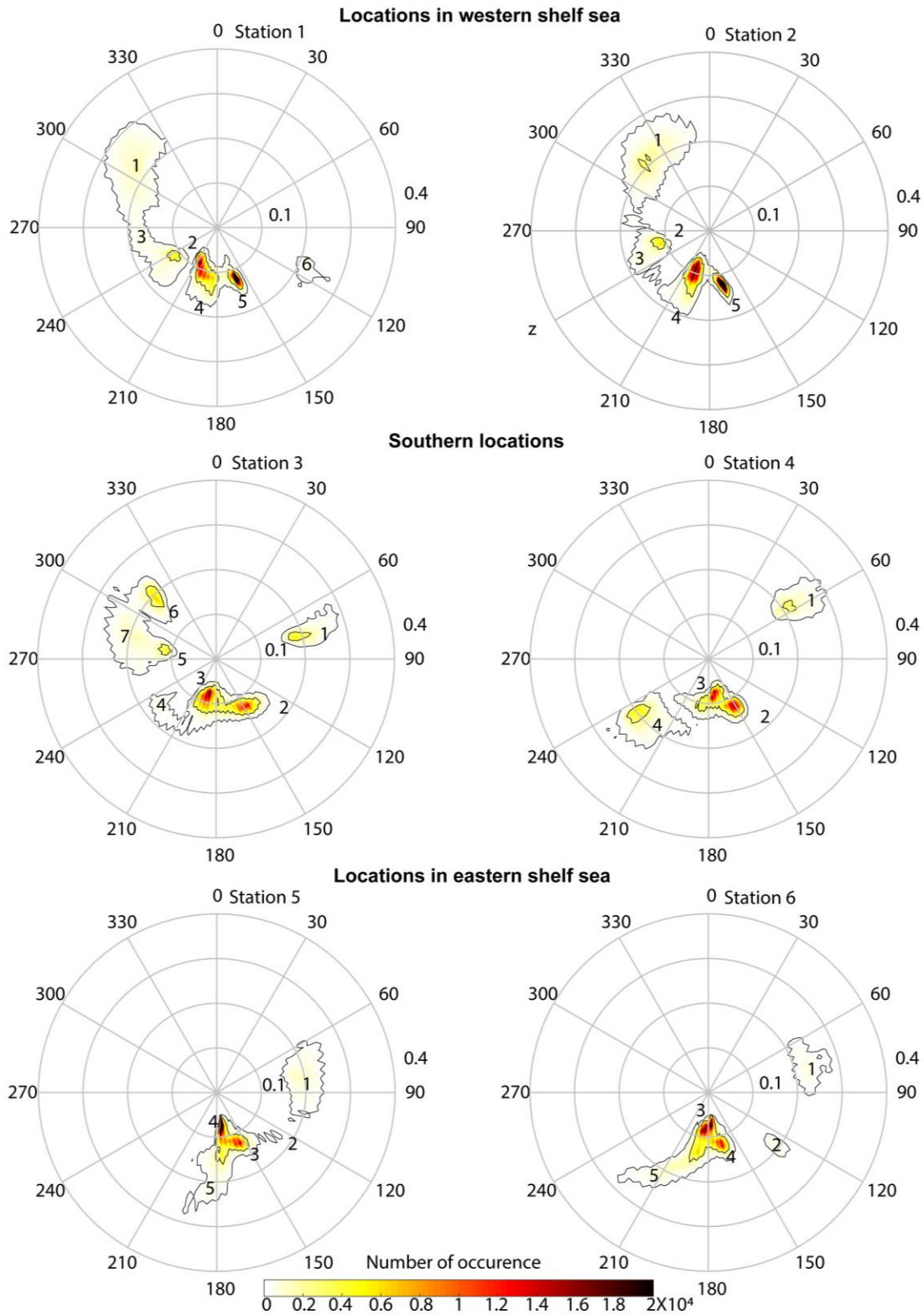


Figure 3. Spectral description of different wave systems with Probability Distribution of Spectral partitions indicated by the color scale for all the stations, where the peak frequency is marked radially on the concentric circles and direction along the outer circle. Frequency ranges from 0 to 0.4 Hz with each concentric circles drawn with spacing of 0.1 Hz

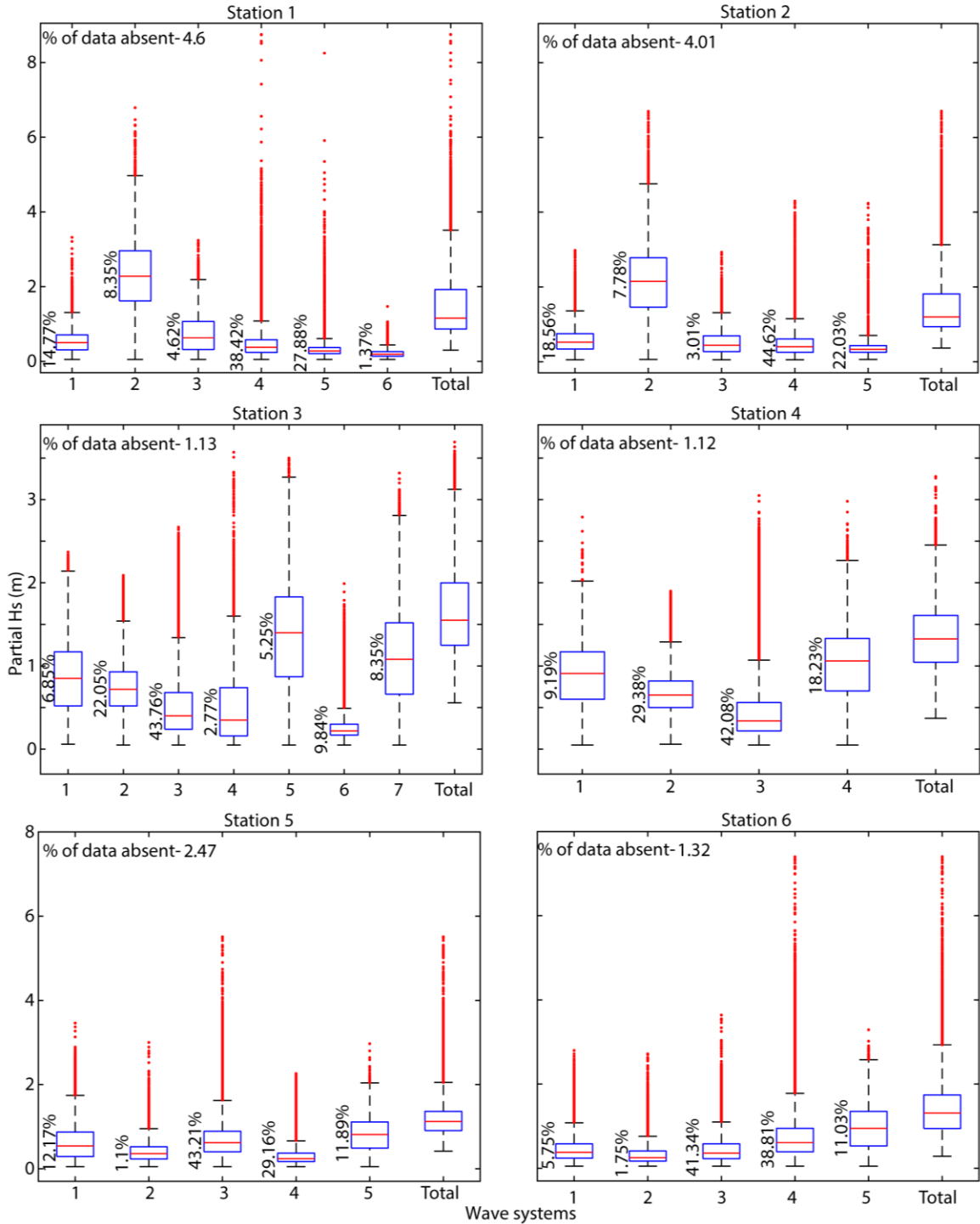


Figure 4. Partial distribution of system wise significant wave height (H_s) at stations 1 to 6. Box indicates the 25th and 75th percentile range (Inter Quartile Range). The whiskers are placed at 1.5 times of interquartile range from the 1st and 3rd quartile values. The outliers fall above this whisker is considered as extremes or tail of the distribution and are given in red dots

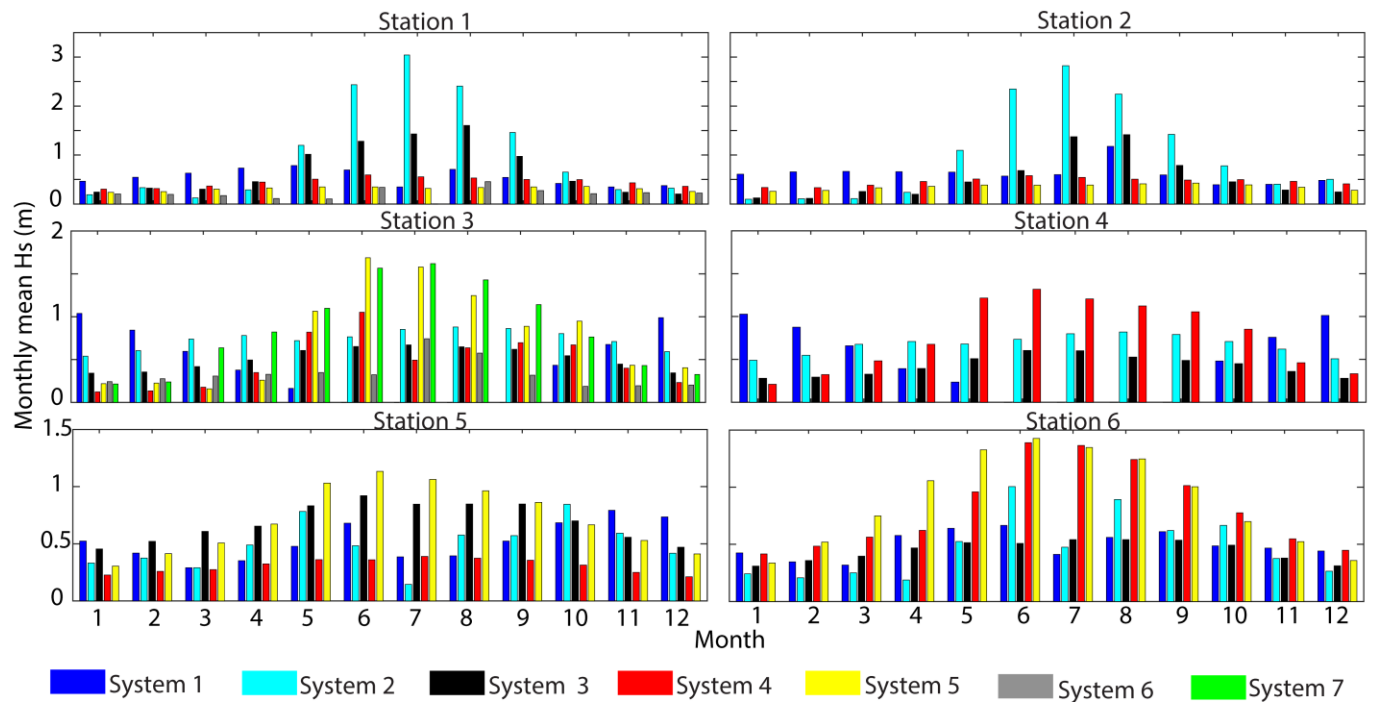


Figure 5. Monthly mean values of partial significant wave height (H_s) of different systems at all the stations

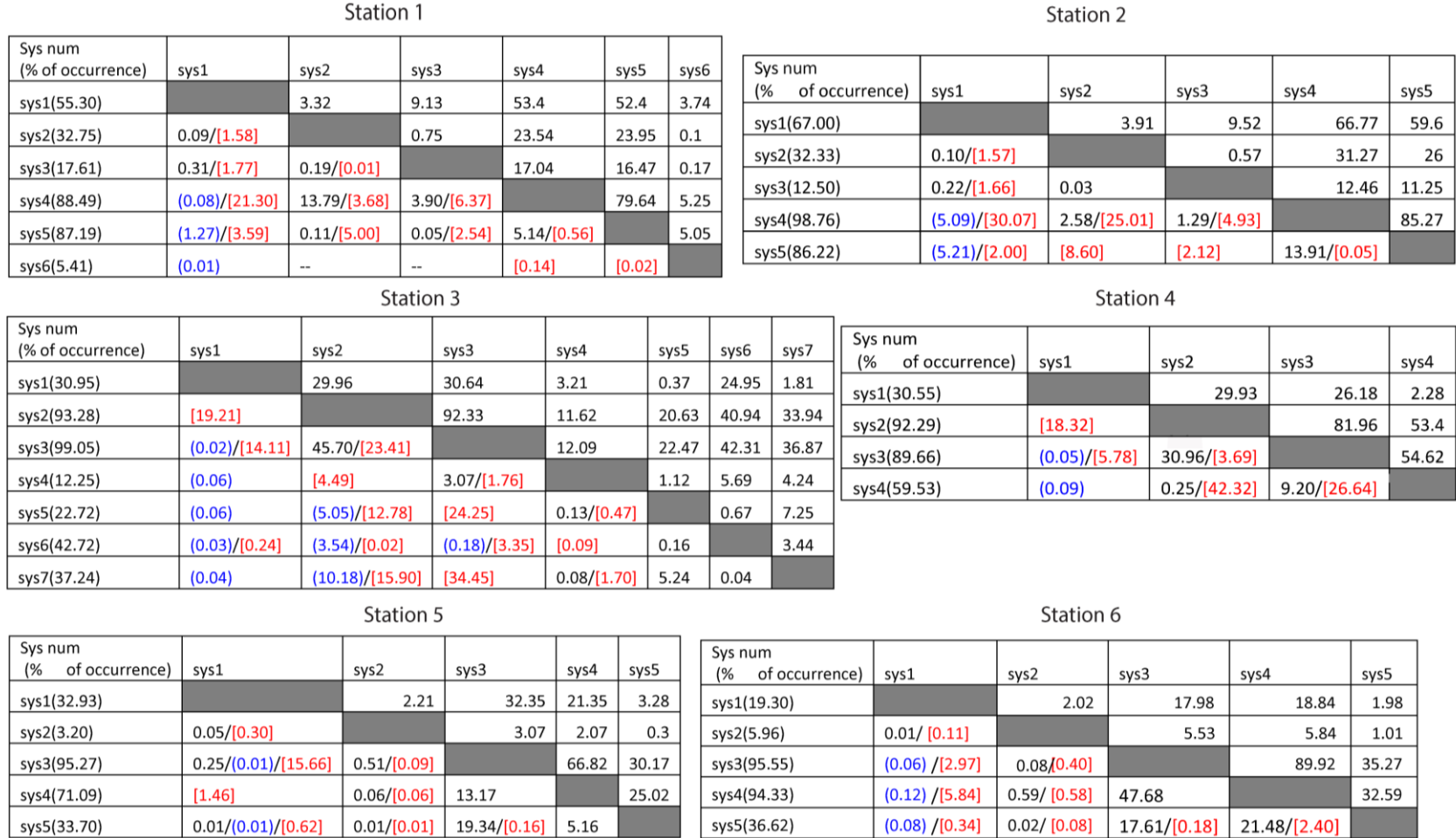


Figure 6. Joint distribution of wave systems at a station with percentage of co-occurrence in the upper half of the table. The percentage of following in black, opposing (blue) and crossing [red] sea states are given in the lower half of the table